Research on Engineering Structures & Materials
www.jresm.org
MIM Research Group

Research Article

Modified strut-and-tie model for predicting shear capacity of continuous deep beams

Ali Mustafa Jalil [*,1,a], Raad Dheyab Khalaf [2,b], Khattab Saleem Abdul-Razzaq [1,c]

[1]*Department of Civil Engineering, Diyala University, Diyala, Iraq*
[2]*Department of Reconstruction and Projects, Diyala University, Diyala, Iraq*

Article Info

Article History:

Received 06 May 2026

Accepted 03 Aug 2026

Keywords:

Continuous deep beams;
Strut and Tie Model;
Struts;
Ties;
Nodes

Abstract

This study aims to establish a Strut-and-Tie model (STM) for calculating the shear strength of continuous deep reinforced concrete beams and is compared with the STM of the ACI 318-25 code. To achieve this, quantitative adjustment coefficients representing the influence of the most important structural factors were introduced. The proposed model is based on differentiating between the effectiveness of internal and external struts, considering the concrete compressive strength, shear span-to-depth ratio, and horizontal and vertical reinforcement ratios. To assess the model's accuracy, a database of 60 continuous deep beams, compiled from previous research, was created. The experimental to theoretical load ratios ranged from 0.86 to 1.22, with the exception of four specimens, which reached values of 1.28 and 1.36, while two others reached 1.40. The statistical results showed that the proposed model achieved a mean value, standard deviation, coefficient of variation, mean absolute error, and coefficient of determination of 1.06, 0.13, 0.12, 100.49 kN, and 0.91, respectively. In comparison, the ACI 318-25 Strut-and-Tie Model recorded corresponding values of 1.23, 0.20, 0.17, 237.33 kN, and 0.49. These results indicate that the proposed model provides closer agreement with the experimental data, with lower scatter and smaller prediction errors than the ACI 318-25 model. However, the coefficient of determination of the ACI 318-25 STM was lower, with an R^2 value of 0.49 compared with 0.91 for the proposed model. This indicates that the proposed model provides better agreement with the experimental results, lower scatter, and improved prediction accuracy.

1. Introduction

Reinforced concrete deep beams with more than two supports are important structural elements that play a role in resisting the high loads applied to them, as shown in Fig. 1a. In this type of beam, the analysis or design equations used for shallow beams cannot be applied, because the sectional strains in deep beams are nonlinear, unlike shallow beams where the strains are linear. Also, shear is considered the governing mode of failure in deep beams, which makes building foundations more vulnerable to differential settlement. This makes their assessment more complicated compared with shallow beams. Therefore, most design codes, especially the ACI 318-25[1], adopt the Strut-and-Tie Method (STM) for the analysis and design of this type of beam. The finite element model proposed by Salman [2], shown in (Fig. 1b), was used to simulate the nonlinear strain distribution, material response, load capacity of the member, and deformation along the beam axis. However, such programs are not simple to use, as they require greater effort, knowledge, and longer processing time, as well as computers with high specifications. Strut-and-Tie Models (STM) provide a simple theoretical approach, as shown in (Fig. 1c), and usually give approximate results that tend

*Corresponding author: eng.alimustafa91@gmail.com
[a]orcid.org/0009-0001-0023-1795; [b]orcid.org/0009-0002-2805-2104; [c]orcid.org/0000-0001-6843-9325
DOI: http://dx.doi.org/10.17515/resm2026-1655st0605rs

to be lower than the actual results through a simplified analysis based on confining and transferring stresses along tension and compression paths, forming a truss model. In this model, the tension members represent the main reinforcement of the deep beam, while the compression members are the struts, which represent the concrete, and the shear reinforcement. These members intersect at nodes where loading is applied, and they are classified as CCC, CCT, or CTT depending on the force paths meeting at the node.

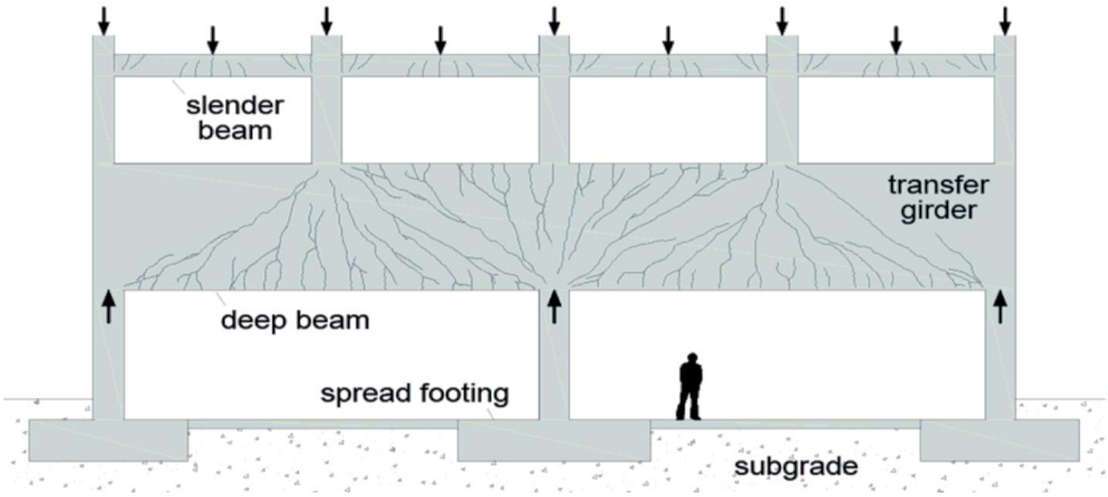

(a) Continuous deep transfer girder in building

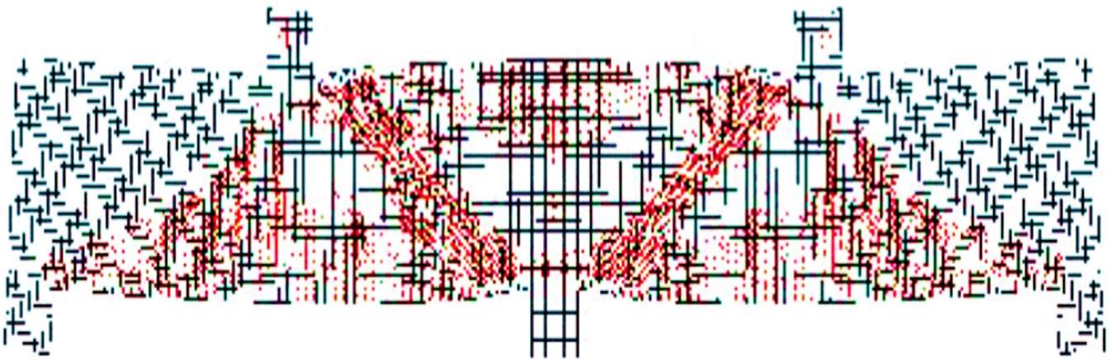

(b) Finite element model of continuous deep beams

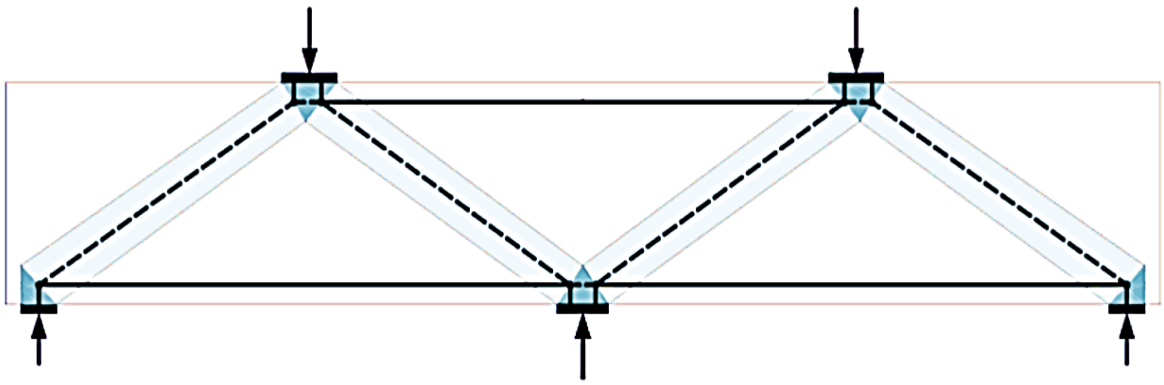

(c) Paths of forces in continuous deep beams

Fig. 1. Modeling of deep transfer girder

The forces are transferred from the nodes and then branch out, with some going toward the compression members and others toward the tension members. The larger part of the load goes toward the inclined compression members. Therefore, they become bottle-shaped and are classified as bottle struts, causing cracks due to tensile stresses in this region. This requires strengthening the region with shear reinforcement to work together with the concrete in resisting the high load carried by the member. Although strut failure is often dominant, reinforcement must also be placed in regions where the tension paths govern. Despite the relative simplicity and strength of this design approach, reinforcement is needed to regulate the flow of stresses along the load paths and to prevent failure of the connecting nodes.

The accuracy of the theoretical analysis depends on the model shape, since a more complex model can be used, that is, one containing a larger number of members and nodes. It also depends on the selected research variables. The strength of the connecting nodes and the strength of the compression members are still under continuous discussion in order to achieve high accuracy in the analysis of deep beams and obtain the best agreement between theoretical and experimental results. A number of researchers have proposed different methods for treating deep beams, including Marti [3], Schlaich et al. [4], MacGregor [5], Abdul-Razzaq et al. [6–12], Jumaa et al. [13], Mohammedali et al. [14], El-Zoughiby et al. [15] and Zhang & Tan [16].

Based on research published in recognized international journals, many widely adopted design codes, such as ACI 318-25 [1], CSA [17], and CEB-FIP Model Code 1990 [18], use different stress values and factors for tension, nodes, and compression. The variation in these values makes it possible to develop a modified STM model with more accurate theoretical results when compared with experimental results. This is very important because these beams are widely used, especially in structures subjected to high and complex loads, and because more accurate calculations are needed in terms of the amount of reinforcement and the dimensions of the model from both the safety and cost perspectives.

2. Adjustment Factor and Shear Reinforcement of the Strut

It is important to understand the direct effect of horizontal and vertical shear web reinforcement resisting inclined stresses in the compressive strut zone on the load-bearing capacity of continuous deep concrete members [19], Figure 2. This is achieved by incorporating the horizontal and vertical shear web reinforcement into the following equations:

$$AVs = 2 * \frac{\pi}{4} * dsv^2 * sin\vartheta * (\frac{w_{e,i}}{sv} + 1) \quad (1)$$

$$AHs = 2 * \frac{\pi}{4} * dsh^2 * cos\vartheta * (\frac{w_{e,i}}{sh} + 1) \quad (2)$$

$$ASe, i = AVs + AHs \quad (3)$$

The participation of the horizontal or vertical reinforcement is transformed along the direction of the internal and external struts in order to determine the actual contribution of the reinforcement in resisting the applied load [20-22]. The contribution of both types of shear web reinforcement to the transfer of external loads through the support is determined through shear reinforcement analysis. Only the reinforcement components in the internal and external strut directions within the strut area subjected to direct compressive stresses from the loading points are considered. The shear web reinforcement component perpendicular to the strut, which resists the strut's tensile stress, is neglected. The reason for neglecting the vertical component is due to the structural nature of the struts. It is classified as a short compression member in which the compressive stresses are dominant and effective.

The yield stress effect was incorporated at a contribution of approximately 50%, since the common failure pattern in deep continuous reinforced concrete beams is sudden (brittle) failure [9]. The strength of the external and internal compressive struts depends on the values of F1 and F2 in addition to the strength of the concrete and steel. These values can be obtained by applying the following equations:

$$For\ external\ strut, Pe = (F_1 . f_{c'} . Ag + 0.5ASe. fy) sin\ \vartheta \quad (4)$$

$$For\ internal\ strut\ Pi = (F_2 . f_{c'} . Ag + 0.5ASi. fy) sin\ \vartheta \quad (5)$$

$$Ptotal = 2(Pe + Pi) \quad (6)$$

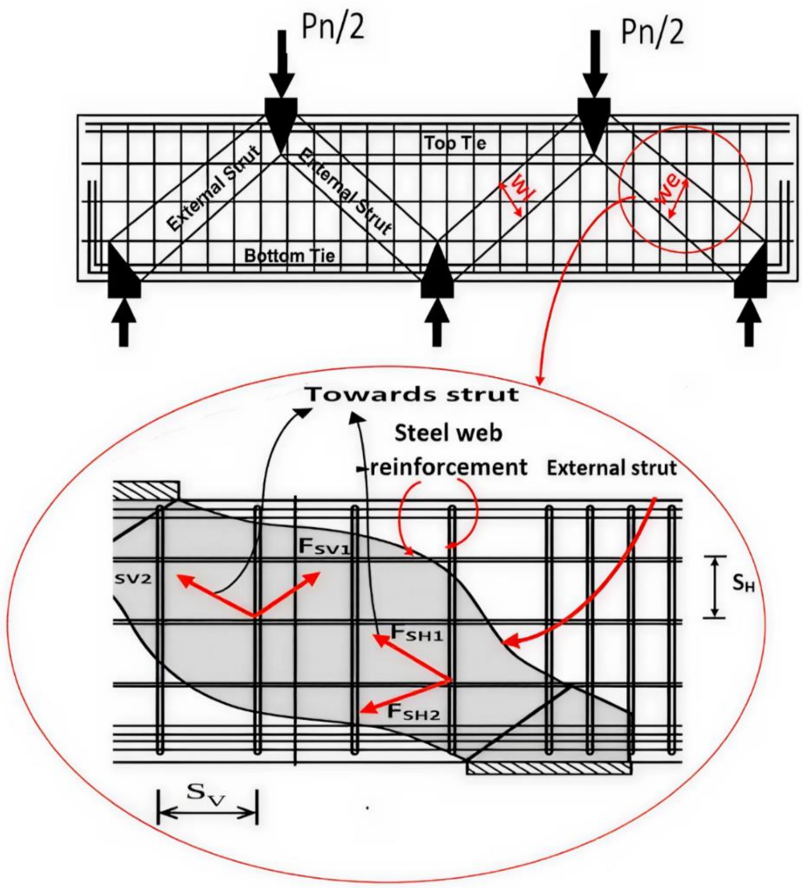

Fig. 2. Contribution of shear strut reinforcement

The two adjustment factors (F_1 and F_2), corresponding to the resistance of the external and internal supports respectively, are assumed to differ typically by approximately 0.25. This distinction is supported by a mechanical rationale associated with the statically indeterminate nature of the structural system, as expressed by Eq. (7) [23]. The internal strut is connected to the middle support, whereas the external strut transfers forces toward the end support. An approximate analysis of the load distribution indicates that the middle support carries nearly 50% of the total applied load, corresponding to approximately 25% contributed by each span, while each end support carries only about 25% of the total load. This difference in load distribution and stress concentration increases the contribution of the internal strut to the overall load-carrying mechanism. Accordingly, the adjustment factor F_2 assigned to the internal strut is taken as 0.25 greater than F_1 for the external strut, thereby providing a more realistic representation of force transfer within two-span continuous deep beams.

$$\textit{Number of truss members} + \textit{Number of reactions} = \textit{Number of equations} \quad (7)$$

A total of 20 two-span continuous deep beams were subjected to an iterative calibration process using a trial-and-error procedure. The calibration was based on four principal variables: the shear span-to-depth ratio, the vertical web-reinforcement ratio, the horizontal web-reinforcement ratio, and the concrete compressive strength.

The calibration strategy initially involved identifying a target value of the adjustment factor F_1, which was found to provide the best mathematical agreement between the experimental and predicted loads. The coefficients associated with the four principal variables in the F_1 equations were then progressively adjusted through repeated iterations. This process continued until the proposed equations produced F_1 values equal, or very close, to the predetermined target value, thereby achieving the best overall agreement between the theoretical predictions and experimental results.

After establishing the final form of the equations, the optimum value of F_1 was substituted into Eq. (4) to calculate the capacity of the external strut. The adjustment factor for the internal strut, F_2, was subsequently determined using Eq. (14) and substituted into Eq. (5) to calculate the internal-strut capacity. Finally, the capacities of the external and internal struts were combined using the general expression given in Eq. (6) to determine the total predicted load capacity. The resulting value was then compared with the experimentally measured ultimate load to assess the accuracy of the proposed model and its suitability for structural applications. The values of F_1 and F_2 are calculated using the following equations:

$(a/h \leq 0.6)$

$$F1 = 0.586 - 298.355\times \rho h - 306.689\times \rho v + 167177.270\times \rho h^2 - 67994.401\times \rho h.\rho v + 163288.696\times \rho v^2 - 18353030.03\times \rho h^3 + 13110177.9\times \rho h^2.\rho v + 13110177.9\, \rho h.\rho v^2 - 18353065.03\, \rho v^3 \quad (8)$$

$(0.6<a/h\leq 1.2,\ f'c\geq 30)$

$$F1 = 0.450 + 31.070\times\rho h + 20.090\times\rho v - 6646.099\times \rho h^2 - 5126.164\times \rho h.\rho v + 4399.483\times \rho v^2 + 244628.297\times \rho h^3 + 172880.200\times \rho h^2.\rho v + 54359.760\times \rho h.\rho v^2 + 4995.704\times \rho v^3 \quad (9)$$

$(0.6<a/h\leq 1.2,\ f'c<30)$

$$F1 = 0.350 - 0.001\times\rho h + 37.496\times\rho v + 0.337\times \rho h.\rho v + 0.150\times \rho v^2 + 0.003\times \rho h^2.\rho v + 0.001\times \rho h.\rho v^2 + 0.001\times \rho v^3 \quad (10)$$

$(a/h>1.2,\ f'c\geq 30)$

$$F1 = 0.600 - 6.667\times\rho h + 10.810\times\rho v + 0.033\times \rho h^2 + 0.065\times \rho h.\rho v + 0.040\times \rho v^2 \quad (11)$$

$(a/h>1.2,\ f'c<30)$

$$F1 = 0.350 + 13.915\times\rho h + 6.184\times\rho v + 0.188\times \rho h^2 + 0.083\times \rho h.\rho v + 0.037\times \rho v^2 + 0.002\times \rho h^3 + 0.001\times \rho h^2.\rho v \quad (12)$$

The following equation, which is less accurate than the previous equations, can also be used.

$$F1 = 2.543472493 - 0.711978694 * a/h - 0.132334722 * f'c + 121.110600747 * \rho h + 28.980270752 * \rho v + 0.465005410 * a/h^2 + 0.002673354 * f'c^2 - 1946.869765635 * \rho h^2 + 6304.244163763 * \rho v^2 - 0.011304047 * a/h.f'c - 83.193452827 * a/h.\rho h + 70.481614698 * a/h.\rho v - 1.213436649 * f'c.\rho h - 2.967831450 * f'c.\rho v + 1552.683604044 * \rho h.\rho v \quad (13)$$

The value of F2 is determined by applying equation below:

$$F_2 = F_1 + 0.25 \quad (14)$$

The proposed method is applicable to continuous deep beams with normal-strength concrete, within the investigated range of a/h ratios corresponding to deep-beam behavior, and for different horizontal and vertical web reinforcement ratios, ρ_h and ρ_v. However, it is not recommended for high-strength concrete, since this concrete class was not included in the calibration range of the model. Fig. 3 illustrates a flowchart procedure for analyzing two continuous deep reinforced concrete beams of equal span.

3. Verification Using a Database of Continuous Deep Reinforced Concrete Beams from Scientific Literature

In the current study, the authors proposed detailed procedures for determining the strength of internal and external compression struts. Several mathematical equations are used to estimate load capacity in an acceptable and reliable manner, as illustrated in the analyzed numerical example in Appendix A. For continuous deep beams with and without web reinforcement, the objective is to ensure that the estimated capacities closely match the experimental or actual loads they encounter. By improving the accuracy of structural analysis and providing a more realistic assessment of the behavior of deep beams under varying loading conditions, the proposed method aims to contribute to better design recommendations for these structural components.

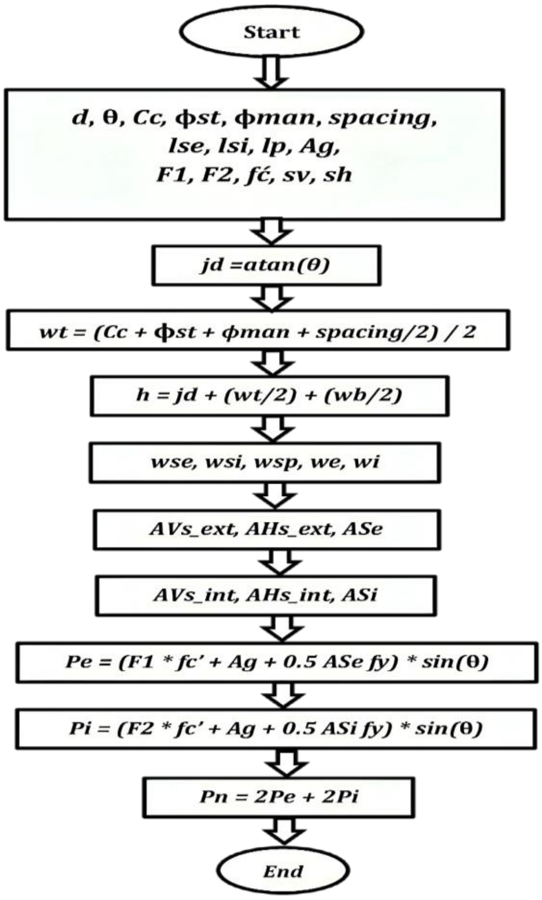

Fig. 3. Flow chart procedure to calculate deep beam capacity

A total of 60 deep, two-span reinforced concrete beams were collected from various references, as shown in Table 1. The beams were tested and collected by different authors [20, 24–31]. The shear span-to-total-depth ratio of the deep beams in the database ranged from 0.5 to 2.0. The test specimens were made of concrete with a compressive strength ranging from 20 to 40 MPa. Some test specimens had no web reinforcement, while others were reinforced with 2% high shear reinforcement. The theoretical load capacity of the test specimens ranged from 483.32 to 2096.27 kN. All beams were reported to have failed in shear due to a large diagonal crack within the internal shear spans.

Table 1. Database of existing specimens and comparison of predicted and measured normalized load capacities

Seq.	Specimen	*a/h* ratio	*Sh* (mm)	*Sv* (mm)	*fć* (MPa)	*P-STM* (kN)	*P-STMmod* (kN)	*P-EXP* (kN)	*P-EXP/ P-STM*	*P-EXP/ P-STMmod*
1.	CR150-35	0.97	60	60	28	713.40	738.81	900	1.26	1.22
2.	CS150-35	0.97	-	-	28	713.40	738.81	945	1.32	1.28
3.	CF150-35	0.97	-	-	28	713.40	738.81	840	1.18	1.14
4.	CR150-50	0.66	60	60	28	892.22	922.08	1100	1.23	1.19
5.	CS150-50	0.66	-	-	28	892.22	922.08	1100	1.23	1.19
6.	CF150-50	0.66	-	-	28	892.22	922.08	1000	1.12	1.08
7.	CR200-50	0.66	60	60	28	952	1203.72	1250	1.31	1.04
8.	CS200-50	0.66	-	-	28	952	1203.72	1200	1.26	1.00
9.	CF200-50	0.66	-	-	28	952	1203.72	1325	1.39	1.10
10.	L5NN	0.50	-	-	32.4	1298	1484.64	1635	1.26	1.10
11.	L5NS	0.50	-	120	32.4	1298	1669.76	1710	1.32	1.02
12.	L5NT	0.50	-	60	32.4	1298	1746.79	1789	1.38	1.02
13.	L5SN	0.50	120	-	32.4	1298	1764.08	1887	1.45	1.07
14.	L5SS	0.50	120	120	32.4	1623	2146.44	2117	1.30	0.99
15.	L5TN	0.50	60	-	32.4	1298	2096.27	2317	1.79	1.11

Seq.	Specimen	a/h ratio	Sh (mm)	Sv (mm)	fć (MPa)	P-STM (kN)	P-STMmod (kN)	P-EXP (kN)	P-EXP/ P-STM	P-EXP/ P-STMmod
16.	L10NN	1.00	-	-	32.1	1000	916.23	880	0.88	0.96
17.	L10NS	1.00	-	120	32.1	1000	1117.89	1153	1.15	1.03
18.	L10NT	1.00	-	60	32.1	1000	1424.07	1541	1.54	1.08
19.	L10SN	1.00	120	-	32.1	1000	1029.28	884	0.88	0.86
20.	L10SS	1.00	120	120	32.1	1250	1166.77	1177	0.94	1.01
21.	L10TN	1.00	60	-	32.1	1000	990.47	935	0.94	0.94
22.	TCDB1-1	1.33	-	-	35.6	1456	1627.10	1595	1.10	0.98
23.	TCDB2-1	1.33	-	-	38.9	1803	1777.93	2000	1.11	1.12
24.	CDB1	1.07	40	100	30	854.23	1080.01	1078	1.26	1.00
25.	CDB2	1.07	80	200	33.1	942.50	933.25	932	0.99	1.00
26.	CDB3	1.07	80	-	22	626.44	578.97	559	0.89	0.97
27.	CDB4	1.07	-	200	28	637.83	842.08	886	1.39	1.05
28.	CDB5	1.07	80	200	28.7	710.61	794.00	804	1.13	1.01
29.	CDB6	1.58	40	100	22.5	423.38	483.32	485.6	1.15	1.00
30.	CDB7	1.58	80	200	26.7	502.41	510.01	436.5	0.87	0.86
31.	CDB8	1.58	80	200	23.6	418.49	410.00	377.7	0.90	0.92
32.	B1	1.03	200	-	31.1	1074	1093.05	1295	1.21	1.18
33.	B2	1.03	200	-	42.5	1466	1587.46	1674	1.14	1.05
34.	B3	1.03	200	-	36	1243	1428.84	1358	1.09	0.95
35.	B7	2.07	-	200	32	500	591.46	579	1.16	0.98
36.	B8	2.07	-	200	38.6	602	766.04	676	1.12	0.88
37.	N4	0.54	-	-	25.8	906.20	1129.45	929.3	1.03	0.82
38.	N8	0.54	-	-	29.6	1039.70	1295.80	1277	1.23	0.99
39.	N13	0.54	-	-	27.4	962.50	1199.49	1466.6	1.52	1.22
40.	N7	0.54	-	-	33.2	1166.20	1453.39	1643.4	1.41	1.13
41.	BS1	1	125	200	20	625.86	719.56	819	1.31	1.14
42.	BS2	1	125	_	20	625.86	556.61	782	1.25	1.40
43.	BS3	1	125	100	20	625.86	862.95	939	1.50	1.09
44.	BS4	0.77	200	_	20	577.30	634.033	889	1.54	1.40
45.	BS5	0.77	200	200	20	721.62	834.48	1001	1.39	1.20
46.	BS6	1	_	200	20	500.69	665.68	735	1.47	1.10
47.	BS7	0.77	130	200	20	721.62	844.42	1145	1.59	1.36
48.	BS8	1.25	75	200	20	511.38	559.90	715	1.40	1.28
49.	BS9	1	125	200	28	876.20	969.65	1015	1.16	1.05
50.	CDBA1	1	-	-	33.81	889.50	925.67	875	0.98	0.95
51.	CDBB1	1	-	150	34.52	908.10	1115.70	992	1.09	0.89
52.	CDBB2	0.5	-	150	34.52	1096.90	1431.40	1288	1.17	0.90
53.	CDBD1	1	110	150	35.12	1154.90	1199.02	1093	0.95	0.91
54.	CDBC1	1	-	150	36.05	948.40	1395.00	1305	1.38	0.94
55.	CDBE1	1	110	150	36.41	1197.3	1397.86	1407	1.18	1.01
56.	L5–40	0.5	_	_	32.4	1147.38	1515.68	1529	1.33	1.01
57.	L5–60	0.5	_	_	32.4	1161.33	1538.54	1635	1.41	1.06
58.	L5–72	0.5	_	_	32.4	1164.64	1544.31	1786.	1.53	1.16
59.	L10–60	1	_	_	32.1	914.88	958.61	880	0.96	0.92
60.	L10–72	1	_	_	32.1	930.14	975.50	1003	1.08	1.03

Note: source-specimens no. 1-9, Abdul-Razzaq et al. [20]; 10-21, K.-H. Yang et al [24]; 22 and 23, N. Zhang and K.-H. Tan [25]; 24-31, A.F. Ashour [26]; 32-36, M.A.T. Khatab et al [27]; 37-40, K.-H. Yang and A. F. Ashour [28]; 41-49, F. B. A. Beshara et al [29];50-55, A. N. Noori and A. F. Ali[30];56-60 , K.-H. Yang, H.-S. Chung, & A. F. Ashour [31]

Fig. 4 and Table 1 illustrate the discrepancy between the experimental and predicted strengths of STM ACI 318-25 code and STM modified for continuous deep beams. The reliability of the analytical model is confirmed by the remarkable agreement between the analytical results and experimental data across several important parameters, such as the compressive strength of plain concrete, the shear span-to-depth ratio, and the horizontal and vertical shear reinforcement ratios. The ratio of the experimental to theoretical values (P-EXP / P-STMmod) ranged from 0.86 to 1.22. with the exception of four specimens, which reached values of 1.28 and 1.36, while two others reached 1.40. This deviation may be attributed to differences in the testing conditions and procedures adopted in the published studies from which the database was compiled, including variations in the loading rate, load-application method, and concrete casting conditions. Since the proposed model was calibrated using a database of 60 specimens to achieve the best overall statistical agreement, a limited number of outliers remained. Nevertheless, these cases did not materially affect the model's overall statistical performance, which demonstrated higher prediction accuracy and lower scatter than the STM specified in ACI 318-25.

Table 2 summarizes the statistical comparison between the ACI 318-25 STM and the modified STM. The modified model showed better prediction accuracy, as the mean value decreased from 1.23 to 1.06, indicating closer agreement with the experimental results and reduced bias. In addition, the standard deviation, coefficient of variation, and MAE decreased from 0.20, 0.17, and 237.33 kN to 0.13, 0.12, and 100.49 kN, respectively. The R^2 value also increased from 0.49 to 0.91, indicating improved agreement between the predicted and experimental values. Overall, these results show that the proposed modifications enhance the prediction performance of the STM for continuous deep beams.

Table 2. Comparison between predicted strengths of ACI 318-25 code STM and modified STM

	Strut and Tie Model by ACI 318-25	Modified Strut and Tie Model
MEAN	1.23	1.06
S.D	0.20	0.13
C.O.V	0.17	0.12
MAE	237.33	100.49
R^2	0.49	0.91

The results show that the adopted theoretical approach for analyzing deep beams simulates the experimental load capacity of the model with high agreement. This provides guidance for the structural engineer in continuously evaluating deep beams and in realistically predicting their shear behavior. It also supports the design and evaluation of concrete structures in an economical manner without unnecessary material consumption, while enhancing the safety of concrete structures.

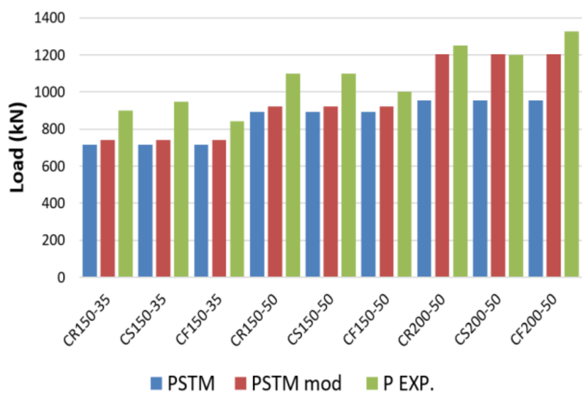

Specimens of Abdul-Razzaq et al. [20]

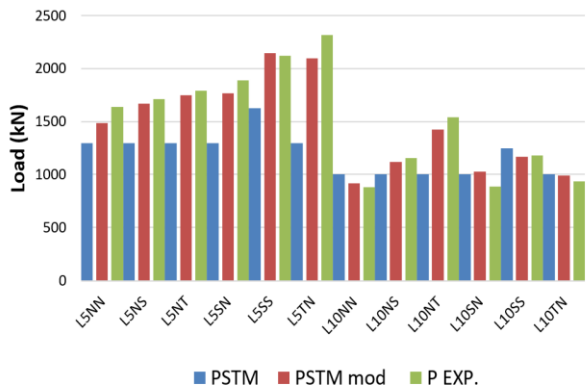

Specimens of K.-H. Yang et al. [24]

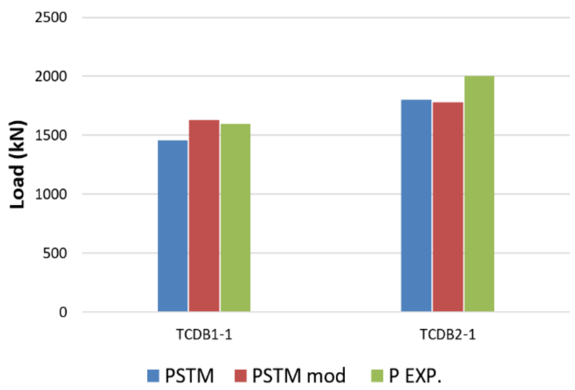

Specimens of N. Zhang and K.-H. Tan [25]

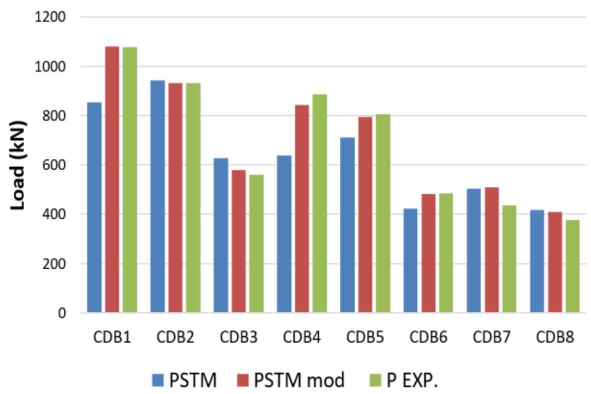

Specimens of A.F. Ashour [26]

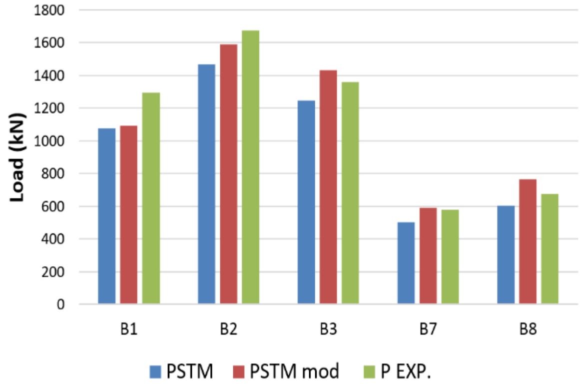

Specimens of M.A.T. Khatab et al. [27]

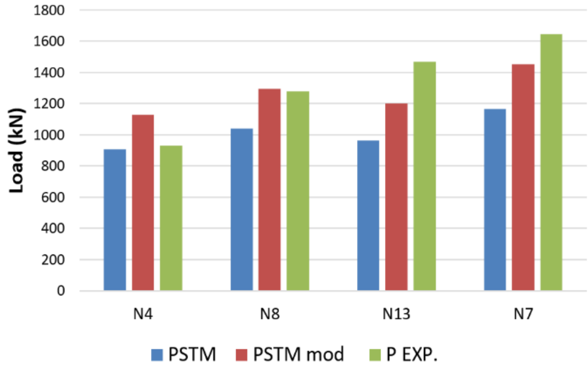

Specimens of K.-H. Yang and A. F. Ashour [28]

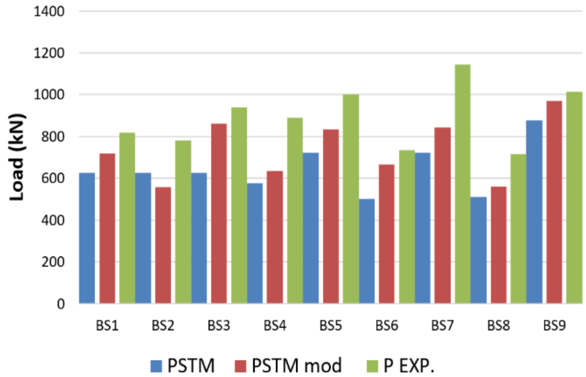

Specimens of F. B. A. Beshara et al. [29]

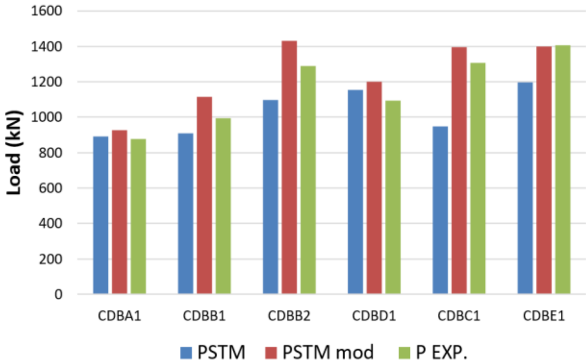

Specimens of A. N. Noori and A. F. Ali [30]

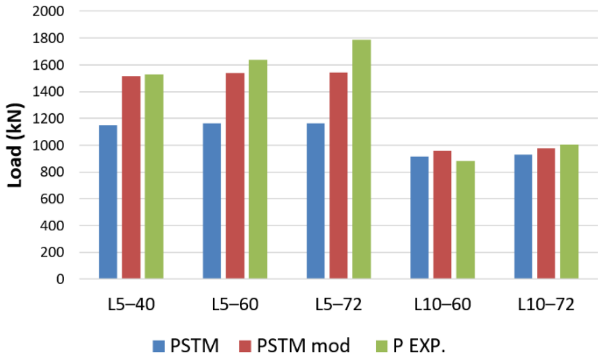

Specimens of K.-H. Yang, H.-S. Chung, & A. F. Ashour [31]

Fig. 4. Comparison between predicted and experimental ultimate load capacity

4. Conclusions

Through comparing the results of the proposed theoretical analysis using the Strut-and-Tie Model (STM) with a set of experimental laboratory data for continuous deep beams reported by previous researchers and published in reputable journals, the method of dealing with deep beams was updated through coefficients and equations governing the paths of shear-stress transfer. The results of the statistical study for analyzing the models can be summarized as follows:

- The proposed STMmod model, which is consistent with the actual stress-transfer paths through the nodes to the tension and compression members, and which is based on the axial distribution of tension and compression forces, provides a suitable practical analytical approach based on the cracking pattern and failure mode of continuous deep beams.

- The adoption of the modification factor F_1 for the outer strut and F_2 for the inner strut contributed significantly to improving the accuracy of the theoretical analysis compared with the experimental test results, since they depend mainly on the shear-span-to-depth ratio (a/h), the horizontal and vertical reinforcement ratios, and the concrete compressive strength ($f'c$).
- The ratio of the experimental load to the theoretical analytical load (P-EXP/P-STMmod) ranged approximately from 0.86 to 1.40, with a mean of 1.06 and a coefficient of variation of about 0.12 for 60 continuous deep beams adopted from previous studies published in reputable journals. These statistics indicate the accuracy of the theoretical analysis in comparison with the experimental load, especially in the case of failure at the inner strut, which is considered the dominant mode in continuous deep beams.
- The proposed model showed improved statistical performance compared with the ACI 318-25 STM. The mean, standard deviation, coefficient of variation, and mean absolute error were reduced by approximately 14%, 35%, 30%, and 58%, respectively, while R^2 increased from 0.49 to 0.91. These results indicate better agreement with the experimental data and lower scatter in the predictions of the proposed model.
- The analysis of the horizontal and vertical shear-reinforcement mesh, and the adoption of its components parallel to the inclined inner and outer struts, together with adopting 50% of the shear-reinforcement stress, showed the actual role of shear reinforcement in reducing the difference between the experimental and theoretical loads and in limiting the occurrence of sudden brittle failure.
- The modified model governs the stress-transfer paths through the inner and outer struts and concentrates the failure of the deep beam through the inner strut, which is consistent with the internal failure observed in the experimental models, since the larger portion of the load travels toward the inner strut in the direction of the middle support. This represents the actual behavior of the stress paths in continuous beams.
- The main variables adopted in the theoretical analysis were the compressive strength of normal- or low-strength concrete, the shear reinforcement ratio, the a/h ratio, and the yield stress of the shear reinforcement, in addition to other variables with less influence. The authors recommend carrying out further studies to include high-strength or high-performance concrete, as well as investigating different loading cases not limited to a concentrated load in each span of continuous beams.
- The proposed analytical model can be a valuable and practical tool for design engineers, combining simple calculations with a good level of accuracy and conservatism in estimating the shear capacity of deep continuous concrete beams, thus contributing to both economical and safe design

Appendix, Numerical Example:

Samples for predictive failure load calculations, based on the modified Strut-and-Tie (STM) method, are presented here for a deep-continuous reinforced concrete beam specimen subjected to a concentrated central loading, tested experimentally by Abdul-Razzaq et al. [20]. The beam has the following dimensions, load, and reinforcement, as shown in (Fig. 5):

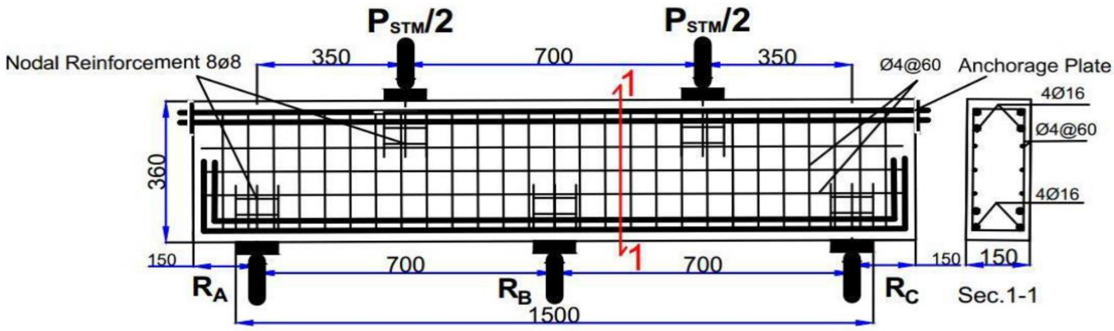

Fig. 5. Two-span continuous deep beam specimen (all dimensions in mm) [20]

h = 360mm, lc=1000mm, d=440.5mm, a=350mm, b_w= 150mm, f'c = 27 MPa, bearing plate dimensions = (100 × 150) mm for external support, middle support and applied load , main longitudinal top and bottom reinforcement = 4ϕ16mm, f_y = 500 MPa, vertical web reinforcement = ϕ4 mm@60 mm c/c, f_{yv}= 500 MPa, horizontal web reinforcement = ϕ4 mm@60 mm c/c, f_{yh}= 500 MPa, bottom and upper covers=25 mm and side cover=15 mm.

$$wt_b = \left(Cc + \emptyset st. + \emptyset main + \frac{spacing}{2}\right) * 2 = (25 + 4 + 16 + 12.5) * 2 = 115\ mm$$
$$wt_b = wt_t = 115\ mm \quad becouse \quad (As_b = As_t)$$
$$jd = h - \frac{wt_t}{2} - \frac{wt_b}{2} = 360 - 115 = 245\ mm$$
$$\vartheta = \tan^{-1}\left(\frac{245}{350}\right) = 35$$
$$w_{se} = wt_b \cos\vartheta + lse \sin\vartheta$$
$$w_{se} = 115 \cos 35 + 100 \sin 35 = 151.6\ mm$$
$$w_{si} = wt_b \cos\vartheta + 0.5lsi \sin\vartheta$$
$$w_{si} = 115 \cos 35 + 0.5 * 100 \sin 35 = 122.9\ mm$$
$$w_{sp} = wt_t \cos\vartheta + 0.5lp \sin\vartheta$$
$$w_{sp} = 115 \cos 35 + 0.5 * 100 \sin 35 = 122.9\ mm$$
$$w_e = \frac{w_{se}}{2} + \frac{w_{sp}}{2} = wt_b \cos\vartheta + \frac{lse + 0.5lp}{2} \sin\vartheta$$
$$w_e = 115 \cos 35 + \frac{100 + 0.5 * 100}{2} \sin 35 = 137.22\ \text{mm}$$
$$w_i = \frac{w_{si}}{2} + \frac{w_{sp}}{2} = wt_b \cos\vartheta + \frac{lsi + lp}{4} \sin\vartheta$$
$$w_i = 115 \cos 35 + \frac{100 + 100}{4} \sin 35 = 122.9\ \text{mm}$$

−For external strut

$$AVs = 2 * \frac{\pi}{4} * dsv^2 * \sin\vartheta * \left(\frac{w_e}{sv} + 1\right) = 2 * \frac{\pi}{4} * 4^2 * \sin 35 * \left(\frac{137.22}{60} + 1\right) = 47.37\ \text{mm}^2$$
$$AHs = 2 * \frac{\pi}{4} * dsh^2 * \cos\vartheta * \left(\frac{w_e}{sh} + 1\right) = 2 * \frac{\pi}{4} * 4^2 * \cos 35 * \left(\frac{137.22}{60} + 1\right) = 67.63\ \text{mm}^2$$
$$ASe = AVs + AHs = 115\ \text{mm}^2$$

−For internal strut

$$AVs = 2 * \frac{\pi}{4} * dsv^2 * \sin\vartheta * \left(\frac{w_i}{sv} + 1\right) = 2 * \frac{\pi}{4} * 4^2 * \sin 35 * \left(\frac{122.9}{60} + 1\right) = 43.93\ \text{mm}^2$$
$$AHs = 2 * \frac{\pi}{4} * dsh^2 * \cos\vartheta * \left(\frac{w_i}{sh} + 1\right) = 2 * \frac{\pi}{4} * 4^2 * \cos 35 * \left(\frac{122.9}{60} + 1\right) = 62.71\ \text{mm}^2$$
$$ASi = AVs + AHs = 106.64\ \text{mm}^2$$

(0.6<a/h≤1.2, f'c<30) → using equation 10 → *F1 = 0.44 and F2=0.69*

$Pe = (F_1 . f_{c'} . Ag + 0.5 ASe . fy) \sin\vartheta =$
(0.44×27×(150×137.22-115)+0.5×115×500)×10³×sin35=157.186 kN

$Pi = (F_2 . f_{c'} . Ag + 0.5 ASi . fy) \sin\vartheta =$
(0.69×27×(150×122.9-106.64)+0.5×106.64×500)×10³×sin35=212.22 kN

$P\_STM_{mod} = 2Pe + 2Pi$=738.8118 kN

Notations

A_{hs}	Area of steel from horizontal shear reinforcement in strut direction, mm^2	a	Shear span measured from support centre to load center, mm
A_{vs}	Area of steel from vertical shear reinforcement in strut direction, mm^2	AS_e	Steel area of internal strut, mm^2
b_w	Width of beam, mm	AS_i	Steel area of internal strut, mm^2
f'_c	150mm×300mm cylinder compressive strength of concrete, MPa	d	Effective depth of beam, distance from centroid of longitudinal tension reinforcement to the extreme compression fibre, mm
F_1	Modification factor of external strut associated with the effect of external support	F_{SH1}	Component of horizontal web reinforcement towards strut

F_2	Modification factor of internal strut associated with the effect of internal support	Cc	Clear cover, mm
f_{yw}	Yield stress of web reinforcement, MPa	Lc	Length of span center to center, mm
j_d	Distance between the centres of the top and bottom nodes, mm	F_{SH2}	Component of horizontal web reinforcement perpendicular strut
P_e	Strength of external strut, kN	F_{SV1}	Compound of vertical web reinforcement towards strut
P_i	Strength of internal strut, kN	F_{SV2}	Compound of vertical web reinforcement perpendicular strut
P-STMmod	Theoretical load failure, kN	H	Overall depth of deep beam, mm
S_h	Spacing of horizontal shear reinforcement, mm	L	Total length of deep beam, mm
S_v	Spacing of vertical shear reinforcement, mm	Ln	Clear length of span, mm
w_{es}	Average effective width of external strut, mm	lp	Length of bearing plate at applied load, mm
w_{is}	Average effective width of internal strut, mm	Lse	Length of external support bearing block, mm
w_{se}	Inclined length for external nodal zone at support, mm	Lsi	Length of internal support bearing block, mm
w_{si}	Inclined length for internal nodal zone at support, mm	ϑ	Angle of inclination of the diagonal compressive stress and the failure plane with the beam longitudinal axis, degree
w_{sp}	Length of inclined internal nodal zone, mm		
w_{spe}	Inclined length for external nodal zone applied load, mm		
w_{spi}	Inclined length for internal nodal zone at applied load, mm		
wt_b	Width of anchor bottom tie, mm		
wt_t	Width of anchor top tie, mm		
Ømain	Diameter of bar for main reinforcement, mm		
Øst	Diameter of bar for shear reinforcement, mm		

References

[1] American Concrete Institute. Building Code Requirements for Structural Concrete (ACI 318-25) and Commentary (ACI 318R-25). Farmington Hills (MI): ACI; 2025.

[2] Salman WD. Nonlinear behavior of reinforced concrete continuous deep beam. Int J Eng Res Technol. 2015;4(4):1139-1145. https://doi.org/10.17577/IJERTV4IS040460

[3] Marti J. Truss models in detailing. J Struct Div. 1977;103:2281-2294. https://doi.org/10.1061/JSDEAG.0004783

[4] Schlaich J, Schäfer K, Jennewein M. Toward a consistent design of structural concrete. PCI J. 1987;32:74-150. https://doi.org/10.15554/pcij.05011987.74.150

[5] MacGregor JG. Reinforced Concrete: Mechanics and Design. 3rd ed. Upper Saddle River (NJ): Prentice-Hall; 1997.

[6] Abdul-Razzaq KS, Dawood AA, Jalil AM. Analysis and design of RC wide corbels: Suggested procedure. AIP Conf Proc. 2020;2213:020112. https://doi.org/10.1063/5.0000050

[7] Abdul-Razzaq KS, Jalil AM, Jebur SF. Behaviour of reinforced concrete deep beams in previous studies. IOP Conf Ser: Mater Sci Eng. 2019;518:022065. https://doi.org/10.1088/1757-899X/518/2/022065
[8] Jalil AM, Hamood MJ, Abdul-Razzaq KS, Mohammed AH. Applying different decentralized loadings on RC continuous deep beams using STM. Int J Civ Eng Technol. 2018;9:2752-2769.
[9] Abdul-Razzaq KS, Jalil AM, Mohammed AH. Applying various types of loading on continuous deep beams using strut and tie modelling. Int J Eng Technol. 2018;7:251-258. https://doi.org/10.14419/ijet.v7i4.20.25935
[10] Abdul-Razzaq KS, Jalil AM. Behavior of reinforced concrete continuous deep beams: Literature review. In: Proceedings of the 2nd Conference of Post Graduate Researches, Al-Nahrain University; 2017; Baghdad, Iraq.
[11] Abdul-Razzaq KS, Dawood AA, Jalil AM. Analysis of unsymmetrical reinforced concrete double corbels. AIP Conf Proc. 2020;2213:020113. https://doi.org/10.1063/5.0000051
[12] Abdul-Razzaq KS, Talal AA, Dawood AA. Role of reinforcement in concrete ring deep beams. ACI Struct J. 2023;120(4):129-141. https://doi.org/10.14359/51737140
[13] Jumaa OW, Noaman AT, Mahmoud AS. Behavior of rubberized concrete deep beams reinforced with GFRP bars. Res Eng Struct Mater. 2025:719-730. http://dx.doi.org/10.17515/resm2025-1228ic1010rs
[14] Mohammedali TK, Jalil AM, Abdul-Razzaq KS, Mohammed AH. STM experimental verification for reinforced concrete continuous deep beams. Int J Civ Eng Technol. 2019;10(2):2227-2239.
[15] El-Zoughiby ME, El-Metwally SE, Al-Shora AT, Agieb EE. Strength prediction of continuous R/C deep beams using the strut-and-tie method. Arab J Sci Eng. 2013;39:1685-1699. https://doi.org/10.1007/s13369-013-0755-2
[16] Zhang N, Tan KH. Direct strut-and-tie model for single span and continuous deep beams. Eng Struct. 2007;29(11):2987-3001. https://doi.org/10.1016/j.engstruct.2007.02.004
[17] Canadian Standards Association. Design of Concrete Structures (CSA A23.3-04). Mississauga (ON): CSA; 2004.
[18] Comité Euro-International du Béton, Fédération Internationale de la Précontrainte. CEB-FIP Model Code 1990. Lausanne: CEB; 1993.
[19] Jalil AM, Khalaf RD, Abdul-Razzaq KS. Efficiency of shear strut factor for reinforced concrete continuous deep beams. IOP Conf Ser: Earth Environ Sci. 2026;1644:012051. https://doi.org/10.1088/1755-1315/1644/1/012051
[20] Abdul-Razzaq KS, Jalil AM, Dawood AA. Reinforcing struts and ties in concrete continuous deep beams. Eng Struct. 2021;240:112339. https://doi.org/10.1016/j.engstruct.2021.112339
[21] Abdul-Razzaq KS, Jebur SF. Suggesting alternatives for reinforced concrete deep beams by reinforcing struts and ties. MATEC Web Conf. 2017;120:01004. https://doi.org/10.1051/matecconf/201712001004
[22] Abdul-Razzaq KS, Ali HI, Abdul-Kareem MM. A new strengthening technique for deep beam openings using steel plates. Int J Appl Eng Res. 2017;12:15935-15947.
[23] Hsieh YY. Elementary Theory of Structures. 3rd ed. Englewood Cliffs (NJ): Prentice-Hall; 1988.
[24] Yang KH, Chung HS, Ashour AF. Influence of shear reinforcement on reinforced concrete continuous deep beams. ACI Struct J. 2007;104:420-429. https://doi.org/10.14359/18772
[25] Zhang N, Tan KH. Effects of support settlement on continuous deep beams and STM modeling. Eng Struct. 2010;32:759-771. https://doi.org/10.1016/j.engstruct.2009.09.019
[26] Ashour AF. Experimental behaviour of reinforced concrete continuous deep beams. Trans Built Environ. 1996;17.
[27] Khatab MAT, Ashour AF, Sheehan T, Lam D. Experimental investigation on continuous reinforced SCC deep beams and comparisons with code provisions and models. Eng Struct. 2017;131:264-274. https://doi.org/10.1016/j.engstruct.2016.11.005
[28] Yang KH, Ashour AF. Aggregate interlock in lightweight concrete continuous deep beams. Eng Struct. 2011;33:572-582. https://doi.org/10.1016/j.engstruct.2010.09.026
[29] Beshara FBA, Shaaban IG, Mustafa TS. Behaviour and analysis of reinforced concrete continuous deep beams. In: Proceedings of the 12th Arab Structural Engineering Conference; 2013 Dec 16-18; Tripoli, Libya. p. 1-13.
[30] Noori AN, Ali AF. Effect of web reinforcement on self-compacting reinforced concrete continuous deep beams. J Eng Sustain Dev. 2018;22(4):211-228. https://doi.org/10.31272/jeasd.2018.4.16
[31] Yang KH, Chung HS, Ashour AF. Influence of section depth on the structural behaviour of reinforced concrete continuous deep beams. Mag Concrete Res. 2007;59(8):575-586. https://doi.org/10.1680/macr.2007.59.8.575